JOURNAL OF CHEMICAL & ENGINEERING DATA

ARTICLE

pubs.acs.org/jced

Removal of Trace Arsenic To Meet Drinking Water Standards Using Iron Oxide Coated Multiwall Carbon Nanotubes

Susana Addo Ntim and Somenath Mitra*

Department of Chemistry and Environmental Science, New Jersey Institute of Technology, Newark, New Jersey 07102, United States

ABSTRACT: This study presents the removal of trace level arsenic to meet drinking water standards using an iron oxide-multiwalled carbon nanotube (Fe-MWCNT) hybrid as a sorbent. The synthesis was facilitated by the high degree of nanotube functionalization using a microwave-assisted process, and a controlled assembly of iron oxide was possible where the MWCNT served as an effective support for the oxide. In the final product, 11 % of the carbon atoms were attached to Fe. The Fe-MWCNT was effective in arsenic removal to below the drinking water standard levels of 10 $\mu g \cdot L^{-1}$. The absorption capacity of the composite was 1723 $\mu g \cdot g^{-1}$ and 189 $\mu g \cdot g^{-1}$ for As(III) and As(V), respectively. The adsorption of As(V) on Fe-MWCNT was faster than that of As(III). The pseudosecond-order rate equation was found to effectively describe the kinetics of arsenic adsorption. The adsorption isotherms for As(III) and As(V) fitted both the Langmuir and Freundlich models.

INTRODUCTION

Arsenic in natural waters is a problem that affects many parts of the world including North America and Asia.[1−3] Arsenic is also listed as a carcinogenic contaminant which is responsible for other health effects such as spontaneous abortion[4] and diabetes.[5] As a result of this, more stringent standards are being established by the United States Environmental Protection Agency (EPA).[6] Typically, arsenite [As(III)], which is neutral, uncharged, and a soluble molecule, is considered more toxic than arsenate or As(V).[7,8] Existing technologies for arsenic removal include oxidation/precipitation, coagulation/coprecipitation, nanofiltration, reverse osmosis, electrodialysis, adsorption, ion exchange, foam flotation, solvent extraction, and bioremediation.[9] Most of these techniques are well-established and have their merits and inherent limitations such as the generation of toxic waste, low arsenic removal efficiencies, and/or high cost.[9]

Adsorption has proven to be an efficient method for arsenic removal, and a wide range of materials including lanthanum/iron compounds, mineral oxides, and biological materials[10] have been studied. The use of polymeric resins, activated carbon, activated alumina, iron-coated sand,[11] hydrous ferric oxide,[12] and natural ores have generated much interest, and novel metal modified adsorbents have demonstrated superior performance.[13,14] At present there is a need for the development of higher capacity sorbents for arsenic removal that will be effective at the trace level so that they may be used for drinking water purification.

Carbon nanotubes (CNTs) are made from graphene sheets seamlessly rolled into cylindrical tubes and are found as single-walled (SWCNT) and multiwall carbon nanotubes (MWCNT), with the latter being relatively inexpensive.[15,16] Their unique characteristics such as a high aspect ratio and superior mechanical, electrical, and thermal properties make them well-suited for many applications. CNTs also exhibit exceptional sorption properties toward various organic compounds and inorganic ions.[17] The potential for sidewall functionalization and surface modification make them attractive as support phases for water treatment.[18−20] Recently we have reported the functionalization of CNTs with tetragonal zirconyl oxide particles, which have proved effective in water defluoridation.[21] A recent study has reported the implementation of a fabric supported magnetite MWCNT composite based supercapacitor for the removal of sodium chloride and arsenic at high $mg \cdot L^{-1}$ levels from seawater.[22] From the standpoint of practical applications, the CNTs can be implemented in water treatment as a replacement for activated carbon with the added advantage that they can be self-assembled on supports via chemical vapor deposition[23] and can also be immobilized in membranes[24] and filters.[22] However, cost and other factors need to be taken into consideration before such a process could be commercialized.

The goal of this project was to synthesize iron oxide-MWCNT using highly functionalized nanotubes and study the removal of $\mu g \cdot L^{-1}$ levels of arsenic from water, to meet the U.S. EPA drinking water standard of 10 $\mu g \cdot L^{-1}$.

EXPERIMENTAL SECTION

Materials and Methods. MWCNTs (OD (20 to 40) nm, purity 95 %) were purchased from Cheap Tubes Inc., and all other chemicals were purchased from Sigma Aldrich with a purity higher than 95 %. Ten $mg \cdot L^{-1}$ stock solutions of As(III) and As(V) were prepared by dissolving weighed amounts of $NaAsO_2$ and Na_2HAsO_4, respectively, in measured volumes of Milli-Q water. The stock solutions were preserved with 1 % trace metal grade HNO_3. A set of 1 $mg \cdot L^{-1}$ working solutions were then prepared from the stock for analysis. pH values were maintained constant during the analysis using 100 mM acetate buffer (pH 4 and 5) and 0.1 M Tris buffer (pH 6 to 8).

The MWCNT was functionalized in a microwave-accelerated reaction system (mode: CEM Mars) fitted with internal temperature and pressure controls according to an experimental

Received: October 20, 2010
Accepted: April 15, 2011
Published: April 27, 2011

dx.doi.org/10.1021/je1010664 | J. Chem. Eng. Data 2011, 56, 2077–2083

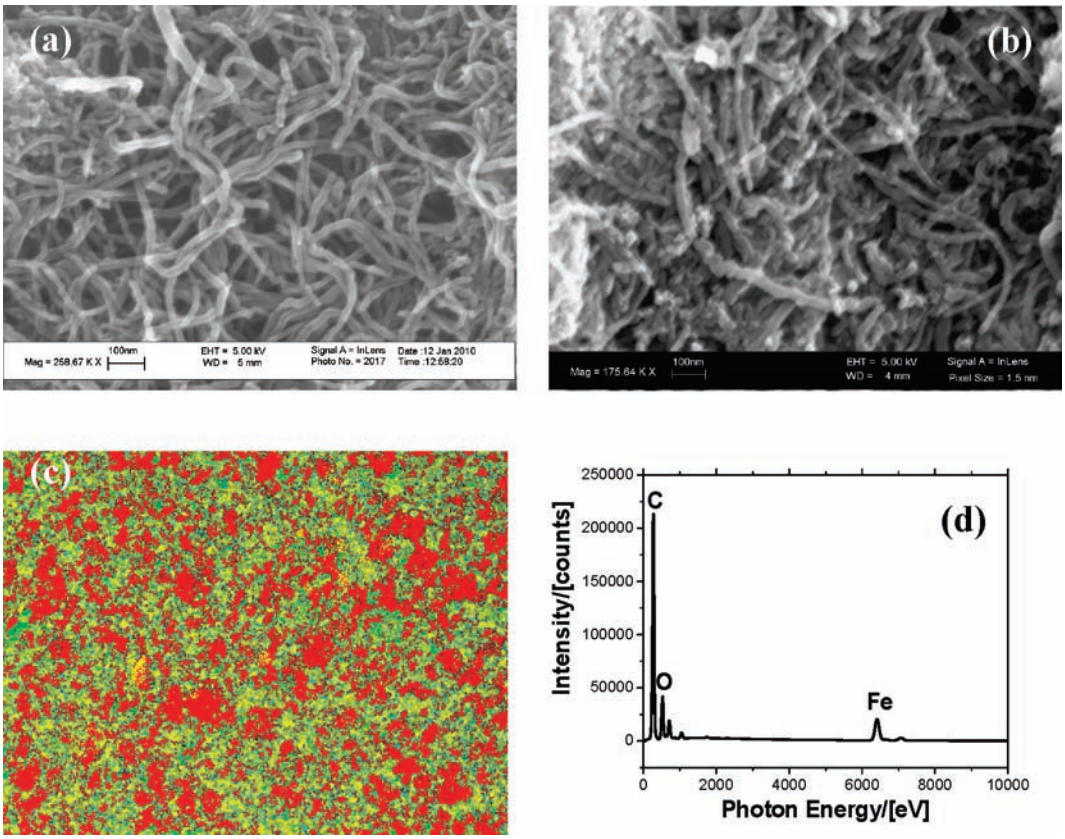

Figure 1. SEM image of (a) acid-functionalized MWCNT, (b) the Fe-MWCNT composite, (c) EDS map (red, carbon; green, oxygen; and yellow, iron), and (d) EDS spectra [carbon (C), oxygen (O), and iron (Fe)].

procedure previously published by our laboratory.[25,26] Preweighed amounts of purified MWCNT were treated with a mixture of concentrated H_2SO_4 and HNO_3 solution by subjecting them to microwave radiation at 120 °C for (20 to 40) min. This led to the formation of carboxylic groups on the surface along with some sulfonation and nitration. The resulting solid was filtered through a 10 μm membrane filter, washed with water to a neutral pH, and dried under vacuum at 80 °C to a constant weight. This product (f-MWCNT) was used in the subsequent synthesis of the Fe-MWCNT composite.

The iron oxide coated (Fe-MWCNT) hybrid was synthesized using a method reported previously.[22,27] This was accomplished by dispersing a weighed amount of the f-MCWNT in a 2:1 aqueous solution of $FeCl_3$: $FeSO_4$ under ultrasonication at room temperature. The dispersion was gently stirred at 70 °C for 5 min, after which 5 M NaOH solution was added and stirred vigorously at 85 °C for 1 h. The pH of the reaction was kept between 5 and 11 with the final pH being 10. The composite thus formed was filtered through a 10 μm membrane filter paper, washed, and acidified to pH 5 with a few drops of 1 M hydrochloric acid and dried under vacuum at 105 °C for 24 h.

The Fe-MWCNT was characterized using a scanning electron microscope (SEM) fitted with an energy dispersive X-ray spectrometer (EDS), thermogravimetric analysis (TGA), Fourier transform infrared spectroscopy (FTIR), and Brunauer−Emmett−Teller (BET) surface area. SEM data were collected on a LEO 1530 VP scanning electron microscope equipped with an energy-dispersive X-ray analyzer. Energy dispersive spectroscopic (EDS) data was collected on the EDAX silicon drift detector (SDD) (Apollo XV) mounted on a Hitachi S-3000N electron microscope with specific light element performance. TGA was performed using a Pyris 1 TGA from Perkin-Elmer Inc. from (30 to 900) °C under a flow of air at 10 mL/min, at a heating rate of 10 °C per min. FTIR measurements were carried out in purified KBr pellets using a Perkin-Elmer (Spectrum One) instrument. The specific surface area, micropore volume, and average pore radius were measured using a Quantachrome NOVA 3000 series (model N32-11) high speed gas sorption analyzer at 77.40 K. Before each experiment, the samples were heated at 180 °C and degassed at this temperature with constant vacuum for four hours. The pH at zero point charge (pH_{zpc}) was determined based on a previously published procedure.[13]

Kinetics and Adsorption Isotherms. A total of 10 mL of 100 $\mu g \cdot L^{-1}$ arsenic solution [As(III) and As(V)] was combined with 0.01 g of the adsorbent in a series of conical flasks, and samples were collected at (5, 10, 15, 30, and 45) min and (1, 3, 6, 12, 15, and 24) h for kinetic studies. The mass of the adsorbent was varied from (0.01 to 0.1) g in the isothermal adsorption studies keeping all other parameters constant (equilibrium contact time 1 and 12 h for As(V) and As(III) respectively and pH 4). The arsenic solutions and the adsorbents were mixed thoroughly at a speed of 175 rpm on a platform shaker (Lab systems Wellmix). The mixture was filtered through a 0.45 μm membrane syringe filter.

Residual arsenic was measured using an Agilent 7500 ICP-MS. All standards were prepared from multielement solution 2A, 10 $mg \cdot L^{-1}$ (Spex Certiprep) with the addition of an internal standard mix (Li,[6] Ge, Y, In, Tb, Bi). A buffer solution was used

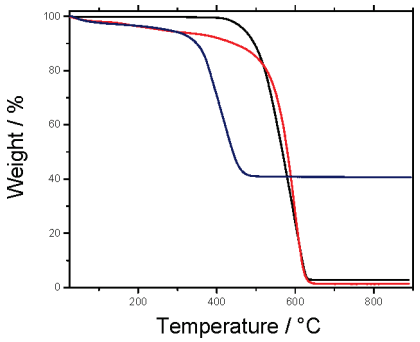

Figure 2. TGA data for MWCNT (black line), f-MWCNT (red line), and Fe-MWCNT (blue line).

for all dilutions. Multielement instrument calibration standard (No. 1, 20 mg/L (Spex Certiprep)) was used for the verification of the calibration.

RESULTS AND DISCUSSION

Sorbent Characterization. The different oxide forms expected in the Fe-MWCNT composite are: magnetite (Fe_3O_4), maghemite (γ-Fe_2O_3), hematite (α-Fe_2O_3), and goethite (α-FeO(OH)).[27] Acid functionalization of the CNTs produced carboxylic groups on the surface, and this enhanced iron oxide loading. The BET surface area of MWCNT and Fe-MWCNT were 110 $m^2 \cdot g^{-1}$ and 153 $m^2 \cdot g^{-1}$, respectively, which shows that the surface area of the CNTs was increased by approximately 40 % with the iron oxide coating. The pH at zero point charge (pH_{zpc}) for MWCNT, f-MWCNT, and Fe-MWCNT were 6.8, 3.91, and 7.35, respectively. This is the point where the surface charge of the CNT is independent of the electrolyte concentration. Therefore, the carboxylic groups on the f-MWCNT had been replaced in the Fe-MWCNT.

SEM images of f-MWCNT and the Fe-MWCNT hybrid are shown in Figure 1. The original MWCNTs had a diameter in the range of (20 to 40) nm, and the length was about (10 to 30) μm. There was no detectable change in tube morphology after acid treatment or iron oxide coating, implying minimal damage to the tube structure. It is quite evident from Figure 1b that, in the case of Fe-MWCNT, the surface was heavily coated with iron oxide.

The EDS data shown in Figure 1c and d also confirmed the presence of relatively large amounts of iron oxide on the surface of the CNTs. TGA was used to quantify the iron oxide loading in the MWCNT as shown in Figure 2a. The resulting weight above 600 °C was attributed to the weight of residual metal or metal oxide. The Fe-MWCNT hybrid was found to contain as much as 40 % (by weight) of iron implying an approximate atomic ratio between Fe and carbon of 11:100. The catalytic activity of the iron is evident from the TGA data, where it altered the thermal stability of the MWCNT. The Fe-MWCNT hybrid degraded at a significantly lower temperature (by nearly 200 °C) compared to the original CNTs, because the iron catalyzed its oxidation, consistent with previous observation.[28]

The IR spectrum (Figure 3) confirmed the presence of functional groups in MWCNT, f-MWCNT, and the Fe-MWCNT hybrid. The carboxylic stretching frequency in f-MCWNT occurred at 1715 cm^{-1} (C═O) and 1218 cm^{-1} (C—O). The stretching (O—H) vibration occurred at 3424 cm^{-1} in the

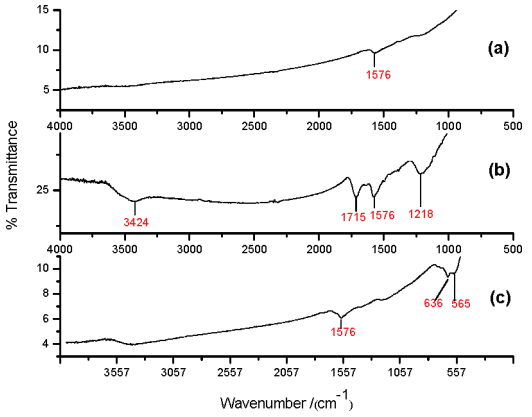

Figure 3. FTIR spectra of (a) MWCNT, (b) f-MWCNT, and (c) Fe-MWCNT.

Table 1. Pseudosecond-Order Kinetic Parameters for As(III) and As(V) Adsorption

	q_e	k_2	h	
	$\mu g \cdot g^{-1}$	$g \cdot (min \cdot \mu g)^{-1}$	$\mu g \cdot (g \cdot min)^{-1}$	R^2
As(III)	97.09	$7.8 \cdot 10^{-4}$	7.35	0.9999
As(V)	103.84	$7.4 \cdot 10^{-3}$	79.79	0.9992

f-MWCNT spectrum (Figure 3b) which is clearly absent from the MWCNT spectrum (Figure 3a). In the Fe-MWCNT spectrum, the characteristic peaks at 1715 cm^{-1}, 1218 cm^{-1}, and 1400 cm^{-1} belonging to the C═O, C—O, and O—H vibrations of carboxylic acid disappear. This may be due to the binding of iron oxide unto the oxidized MWCNT surface. On the basis of the disappearance of the C—O and O—H peaks, it is evident that the iron oxide particles are anchored to the MWCNTs by an ester-like bond.[29] In all of the samples, the peak around 1576 cm^{-1} was assigned to the C═C stretching of the carbon skeleton. The appearance of two new bands at (636 and 565) cm^{-1} in (c) confirmed the formation of the Fe—O bonds.

Arsenic Removal and Its Kinetics. The arsenic removal capacity of Fe-MWCNT was compared to those of the original MWCNTs and functionalized multiwall carbon nanotubes (f-MWCNT). The adsorption capacity for arsenic shown by Fe-MWCNT for both As(III) and As(V) (1723 $\mu g \cdot g^{-1}$ and 189 $\mu g \cdot g^{-1}$, respectively) was much higher than the values obtained for MWCNT (10 $\mu g \cdot g^{-1}$ and 23 $\mu g \cdot g^{-1}$, respectively) and f-MWCNT (3 $\mu g \cdot g^{-1}$ and 9 $\mu g \cdot g^{-1}$, respectively). The adsorption capacity for As(III) and As(V) using Fe-MWCNT was also found to be higher than that for iron coated sand,[11,30,31] ferrihydrite,[31] and hardened paste of Portland cement.[32] It was higher than the values reported for iron oxide-coated biomass[33] but much less than those shown by activated carbon and activated alumina, mostly due to the fact that the initial concentrations of arsenic in these studies were as high as 100 $mg \cdot L^{-1}$.

Oxyanionic arsenic species such as arsenate and arsenite adsorb at the iron oxyhydroxide surface by forming complexes with the surface sites.[34] This assertion is supported by the poor adsorption capacities obtained from analysis with MWCNT and f-MCWNT. As(V) and As(III) showed different sorption

dx.doi.org/10.1021/je1010664 |J. Chem. Eng. Data 2011, 56, 2077–2083

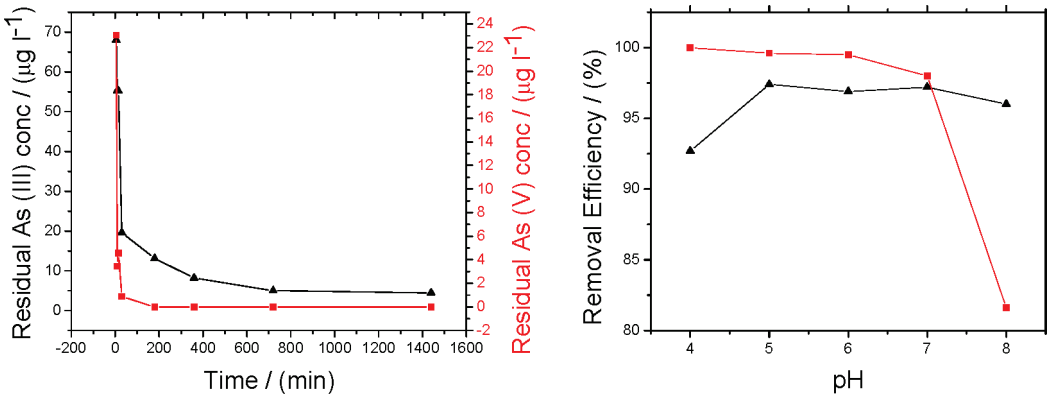

Figure 4. (a) Residual arsenic concentration as a function of time and (b) effect of pH on As(III) and As(V) adsorption. Symbols: ▲, As(III); ■, As(V).

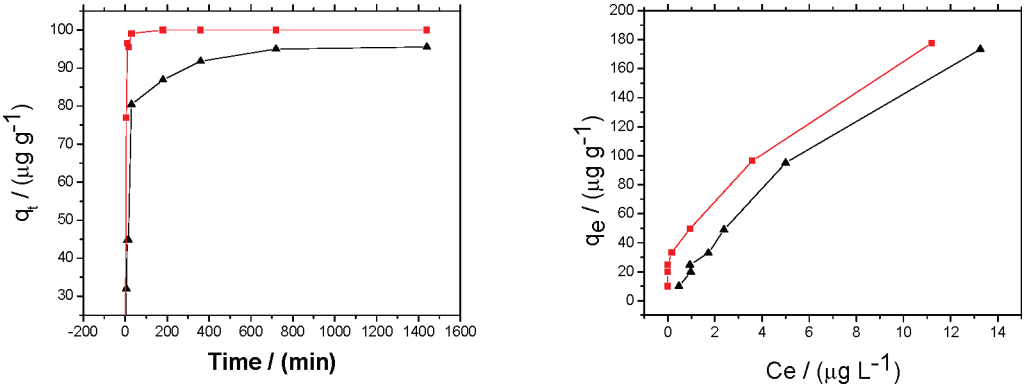

Figure 5. Kinetic and equilibrium data at pH 4 for As(III) and As(V) adsorption by Fe-MWCNT. Symbols: ▲, As(III); ■, As(V).

behavior as can be seen from the isothermal and kinetic data. This difference in their sorption characteristics may be due to their ionic forms at a pH of 4. In the pH range studied, As(V) existed in the anionic form $H_2AsO_4^-$, whereas As(III) is partially ionized below pH 9.22, existing in the molecular form (H_3AsO_3). This may account for the better adsorption of As(V) compared to As(III). Anionic arsenic species ($H_2AsO_3^-$, $H_2AsO_4^-$) are reported to be adsorbed with the positively charged iron oxide-coated adsorbents through electrostatic attraction. There are also reports of the surface potential of iron loaded adsorbents becoming less negative with increasing iron loading.[35] We therefore postulate that arsenic removal with Fe-MWCNT may occur via multiple mechanisms. Negatively charged arsenic species may adsorb onto positively charged sites on the adsorbent surface resulting in their removal from water.

When the iron oxide was exposed to water, metal ions on the oxide surface completed their coordination shells with OH groups,[36] which either bound to or released H^+ ions depending on the pH, and in the process developed a surface charge. The adsorption properties of oxides are due to the existence of these OH_2^+, OH, and O^- functional groups.[37] Arsenic may be removed by ligand exchange with OH and OH_2^+ functional groups on the surface forming an inner-sphere complex. An incompletely dissociated acid $H_2AsO_4^-$ is required to provide a proton for complexation with the OH group to form H_2O and providing space for anion adsorption.[36] Therefore, arsenic species may be removed through complexation with oxyhydroxide sites on the adsorbent surface according to eqs 1 and 2.[33]

$$\alpha\text{-FeOOH} + H_2AsO_4^- + 3H^+ \rightarrow FeH_2AsO_4 + 2H_2O \quad (1)$$

$$\alpha\text{-FeOOH} + H_3AsO_3 + 2H^+ \rightarrow FeH_2AsO_3 + 2H_2O \quad (2)$$

The kinetics of arsenic uptake was investigated by the Lagergren[38] and Ho and McKay[39] kinetic models. Lagergren models the rate of adsorption of pollutants on an adsorbent after a pseudofirst-order equation:

$$\frac{dq_t}{dt} = k_1(q_e - q_t) \quad (3)$$

where q_e and q_t are the sorption capacity ($\mu g \cdot g^{-1}$) of the adsorbent at equilibrium and at time t (h), respectively, and k_1 is the pseudofirst-order sorption rate constant (h^{-1}). Ho and McKay proposed a pseudosecond-order equation of the form:

$$\frac{dq_t}{dt} = k_2(q_e - q_t)^2 \quad (4)$$

where k_2 is the pseudosecond-order sorption rate constant ($g \cdot h \cdot \mu g^{-1}$) and t is time (h). Figure 5a shows the residual As(III) and As(V) concentrations versus time at pH 4. After 10 min of contacting the adsorbent with 100 $\mu g \cdot L^{-1}$ Arsenic solution, 96 % of As(V) was removed, whereas only 45 % of As(III) was removed. 99 % of As(V) and 80 % of As(III) were removed after 30 min of contact. Ho and McKay's pseudosecond kinetic equation was a better fit for adsorption of both As(III)

dx.doi.org/10.1021/je1010664 |J. Chem. Eng. Data 2011, 56, 2077–2083

Table 2. Adsorption Isotherm Parameters for Removal of As(III) and As(V) by Fe-MWCNT

	Langmuir			Freundlich		
	q_m	b		K_f		
	$\mu g \cdot g^{-1}$	$L \cdot \mu g^{-1}$	R^2	$L \cdot \mu g^{-1}$	n	R^2
As(III)	1723	0.013	0.9899	21.89	1.181	0.9907
As(V)	189	0.373	0.9900	50.83	1.946	0.9997

and As(V) than the Lagergren's pseudofirst-order equation. The pseudosecond-order kinetic parameters for As(III) and As(V) removal are presented in Table 1. The R^2 values for both As(III) and As(V) were close to unity implying that their adsorption can best be described by the pseudosecond-order kinetic model with chemisorption being the rate-limiting step. This means that the adsorption rate is proportional to the amount of adsorbent and the square of the number of free sites. The latter corresponds to the term $(q_e - q_t)^2$ in the pseudosecond-order model.

The rate of As(V) removal was faster than that of As(III) as shown by the pseudosecond-order kinetic parameters in Table 1. The higher removal rate of As(V) relative to As(III) may be due to the easy formation of ferric arsenate.[40] Faster adsorption of arsenate than arsenite has also been attributed to the smaller radius of the arsenate ion [(4.0 to 4.2) Å] compared with that of the arsenite ion (4.8 Å).[41]

The optimum pH for As(V) removal was determined to be 4; the equilibrium adsorption q_e ($\mu g \cdot g^{-1}$) of As(V) was found to decrease slightly from pH 4 through 8 as presented in Figure 4b. On the contrary the equilibrium adsorption of As(III) was found to increase slightly from pH 4 to pH 6 and remained constant from pH 6 to pH 8 (Figure 4b). As(III) is dominant in the form of neutral species (H_3AsO_3) below pH 9.22, accounting for the relatively constant As(III) adsorption. A reduced removal of As(V) at pH 8 may be because OH^- ion becomes dominant at an alkaline pH, and this ion competes with arsenic species [$H_2AsO_4^-$]. The pH range studied here was within what is normally encountered in water resources.

Adsorption Isotherms for As(III) and As(V) Removal. The capacity of arsenic removal by the adsorbent was evaluated with the Langmuir[42] and Freundlich[43] isotherms. The linear form of the Langmuir adsorption isotherm is presented below;

$$\frac{1}{q_e} = \frac{1}{q_m} + \frac{1}{bq_mC_e} \quad (5)$$

where q_m ($\mu g \cdot g^{-1}$) is the maximum sorption capacity for monolayer coverage of the adsorbent, C_e ($\mu g \cdot L^{-1}$) is the equilibrium concentration of arsenic, and the Langmuir constant b ($L \cdot \mu g^{-1}$) is indirectly related to the enthalpy of adsorption. The linearized form of the Freundlich isotherm involves a plot of log q_e and log C_e with n and log k_f being the slope and y-intercept, respectively.

$$\log q_e = \log k_f + 1/n \log C_e \quad (6)$$

The Freundlich constants k_f and $1/n$ measure the adsorption capacity and intensity, respectively. The bond energy increases proportionally with surface density for $n < 1$ and vice a versa for $n > 1$.

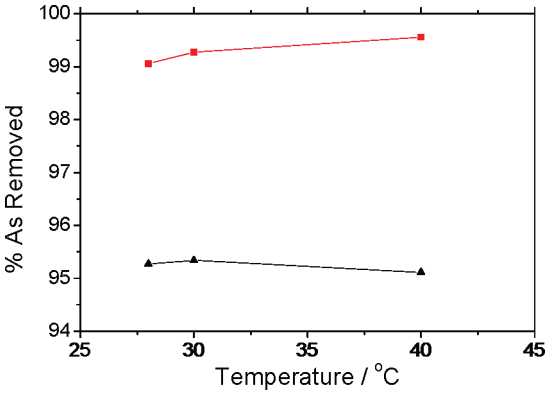

Figure 6. Arsenic removal efficiency as a function of temperature. Symbols: ▲, As(III); ■, As(V).

The Langmuir isotherm parameters presented in Table 2 indicate a high maximum sorption capacity for monolayer adsorption (q_m) for the adsorbent in the removal of As(III). The adsorption of As(III) and As(V) fit both the Langmuir and the Freundlich equations; however, the coefficient of determination (R^2) value for the Freundlich model in both instances were higher than that of the Langmuir equation. Hence the Freundlich isotherm model effectively explained the removal of As(III) and As(V) by the adsorbent with coefficient of determination (R^2) values of 0.9907 and 0.9997, respectively.

The Freundlich constants log k_f and n were obtained from the y-intercept and slope, respectively. The constants k_f ($mg \cdot g^{-1}$) and $1/n$ provide a measure of adsorption capacity and intensity, respectively, and are presented in Table 2. The bond energy increases proportionally with surface density for $n < 1$ and vice versa for $n > 1$.[43] The adsorption capacity for the adsorbent in As(V) removal was much higher than As(III) as was the intensity. The Freundlich isotherm model effectively explained the removal of As(V) by the adsorbent with a coefficient of determination of 0.9995. The value of the constant $1/n$ (0 to 1) is also indicative of the heterogeneity of the adsorbent surface, with $1/n$ closer to 0 implying a heterogeneous surface. The kinetic and equilibrium data at pH 4 for As(III) and As(V) adsorption are shown in Figure 5.

Effect of Temperature on Arsenic Removal. The effect of temperature on arsenic removal efficiency was investigated at pH 4, 1 $g \cdot L^{-1}$ adsorbent dose, 180 rpm agitation, and (1 and 12) h equilibration time for As(V) and As(III), respectively. The temperature was varied from (28 to 40) °C. It was found that arsenic removal efficiency was fairly constant over the temperature range. A plot of arsenic removal versus temperature is presented in Figure 6. A study using Fe^{3+}-impregnated granular activated carbon (GAC) reported a decrease in arsenic As(III) and As(V) removal efficiency with increasing temperature from (30 to 60) °C,[44] but the decrease did not seem substantial.

■ CONCLUSION

A Fe-MWCNT hybrid was effective as a sorbent material for arsenic removal from water. Controlled assembly of iron oxide was possible, and the MWCNT served as an effective support for the oxide. The kinetics of As(III) and As(V) removal was explained by the pseudosecond-order rate equation and their adsorption by the Langmuir and Freundlich models. It is

conceivable that MWCNT with appropriate surface modification can provide a platform for developing potentially useful environmental remediation tools.

AUTHOR INFORMATION

Corresponding Author

*E-mail: mitra@njit.edu. Tel.: +01 973 596 5611. Fax: +01 973 596 3586.

Funding Sources

Partial financial support for this work was provided by the National Institute of Environmental Health Sciences (NIEHS) under Grant No. RC2 ES018810 and the Schlumberger Foundation through the faculty for the future fellowship.

ACKNOWLEDGMENT

The authors would like to thank Dr Yuhong Chen for helping with the EDS analysis and Dr. Larisa Krishtopa for helping with the ICP-MS analysis.

REFERENCES

(1) Mondal, P.; Majumder, C. B.; Mohanty, B. Laboratory based approaches for arsenic remediation from contaminated water: Recent developments. *J. Hazard. Mater.* **2006**, *137* (1), 464–479.

(2) Chatterjee, A.; Das, D.; Mandal, B. K.; Chowdhury, T. R.; Samanta, G.; Chakraborty, D. Arsenic in ground water in six districts of West Bengal, India: the biggest arsenic calamity in the world. Part I. Arsenic species in drinking water and urine of the affected people. *Analyst* **1995**, *120*, 643–656.

(3) Dhar, R. K.; Biswas, B. K.; Samanta, G.; Mandal, B. K.; Chakraborti, D.; Roy, S.;Groundwater arsenic calamity in Bangladesh. *Curr. Sci.* **1997**, *73* (1), 48–59.

(4) Richardson, S. D. Environmental mass spectrometry: Emerging contaminants and current issues. *Anal. Chem.* **2006**, *78* (12), 4021–4045.

(5) Navas-Acien, A.; Silbergeld, E. K.; Pastor-Barriuso, R.; Guallar, E. Arsenic Exposure and Prevalence of Type 2 Diabetes in US Adults. *J. Am. Med. Assoc.* **2008**, *300* (7), 814–822.

(6) *Federal Register No. 14*, Vol. *66*; U.S. Environmental Protection Agency (EPA): Washington, DC, 2001; pp 6976−7066.

(7) Knowles, F. C.; Benson, A. A. The biochemistry of arsenic. *Trends Biochem. Sci.* **1983**, *8* (5), 178–180.

(8) Pattanayak, J.; Mondal, K.; Mathew, S.; Lalvani, S. B. A parametric evaluation of the removal of As(V) and As(III) by carbon based adsorbents. *Carbon* **2000**, *38*, 589–596.

(9) Mohan, D.; Pittman, C. U., Jr. Arsenic removal from water/waste water using adsorbents - a critical review. *J. Hazard. Mater.* **2007**, *142*, 1–53.

(10) Elizalde-González, M. P.; Mattusch, J.; Einicke, W.-D.; Wennrich, R. Sorption on natural solids for arsenic removal. *Chem. Eng. J.* **2001**, *81*, 187–195.

(11) Thirunavukkarasu, O. S.; Viraraghavan, T.; Subramanian, K. S. Arsenic removal from drinking water using iron oxide-coated sand. *Water, Air, Soil Pollut.* **2003**, *142*, 95–111.

(12) Wilkie, J. A.; Hering, J. G. Adsorption of arsenic onto hydrous ferric oxide: effects of adsorbate/adsorbent ratios and co-occurring solutes. *Colloids Surf., A* **1996**, *107*, 97–110.

(13) Chen, W. F.; Parette, R.; Zou, J. Y.; Cannon, F. S.; Dempsey, B. A. Arsenic removal by iron-modified activated carbon. *Water Res.* **2007**, *41*, 1851–1858.

(14) Schmidt, G. T.; Vlasova, N.; Zuzaan, D.; Kersten, M.; Daus, B. Adsorption mechanism of arsenate by zirconyl-functionalized activated carbon. *J. Colloid Interface Sci.* **2008**, *317*, 228–234.

(15) Iijima, S. Helical microtubules of graphitic carbon. *Nature* **1991**, *354*, 56–58.

(16) Iijima, S. Carbon nanotubes: past, present, and future. *Phys. B* **2002**, *323*, 1–5.

(17) Tojanowicz, M. Analytical applications of carbon nanotubes: a review. *Trends Anal. Chem.* **2006**, *25* (5), 480–489.

(18) Wang, Y.; Iqbal, Z.; Mitra, S. Microwave-induced rapid chemical functionalization of single-walled carbon nanotubes. *Carbon* **2005**, *43*, 1015–1020.

(19) Wang, Y.; Iqbal, Z.; Mitra, S. Rapid, low temperature microwave synthesis of novel carbon nanotube-silicon carbide composite. *Carbon* **2006**, *44* (13), 2804–2808.

(20) Wang, Y.; Iqbal, Z.; Mitra, S. Rapidly functionalized, water-dispersed carbon nanotubes at high concentration. *J. Am. Chem. Soc.* **2006**, *128* (1), 95–99.

(21) Sai Sathish, R.; Chen, Y.; Kalyan, M. K.; Nageswara Rao, G.; Janardhana, C.; Mitra, S. Carbon nanotube-zirconium dioxide hybrid for defluoridation of water. *J. Nano Sci. Nano Technol.* **2011**, *11*, 3552−3559.

(22) Mishra, A. K.; Ramaprabhu, S. Magnetite Decorated Multiwalled Carbon Nanotube Based Supercapacitor for Arsenic Removal and Desalination of Seawater. *J. Phys. Chem. C* **2010**, *114*, 2583–2590.

(23) Karwa, M.; Iqbal, Z.; Mitra, S. Scaled-up self-assembly of carbon nanotubes inside long stainless steel tubing. *Carbon* **2006**, *44* (7), 1235–1242.

(24) Hylton, K.; Chen, Y.; Mitra, S. Carbon nanotube mediated microscale membrane extraction. *J. Chromatogr., A* **2008**, *1211* (1−2), 43–48.

(25) Chen, Y.; Iqbal, Z.; Mitra, S. Microwave-Induced Controlled Purification of Single-Walled Carbon Nanotubes without Sidewall Functionalization. *Adv. Funct. Mater.* **2007**, *17*, 3946–3951.

(26) Chen, Y.; Mitra, S. Fast microwave-assisted purification, functionalization and dispersion of multi-walled carbon nanotubes. *J. Nanosci. Nanotechnol.* **2008**, *8* (11), 5770–5775.

(27) Zhang, Q. L.; Lin, Y. C.; Chenc, X.; Gao, N. Y. A method for preparing ferric activated carbon composites adsorbents to remove arsenic from drinking water. *J. Hazard. Mater.* **2007**, *14*, 671–678.

(28) Brukh, R.; Mitra, S. Kinetics of carbon nanotube oxidation. *J. Mater. Chem.* **2007**, *17*, 619–623.

(29) Yan, S.; Lian, G. Synthesis and characterization of phase controllable ZrO_2−carbon nanotube nanocomposites. *Nanotechnology* **2005**, *16*, 625–630.

(30) Gupta, V. K.; Saini, V. K.; Jain, N. Adsorption of As(III) from aqueous solutions by iron oxide-coated sand. *J. Colloid Interface Sci.* **2005**, *228* (1), 55–60.

(31) Thirunavukkarasu, O. S.; Viraraghavan, T.; Subramanian, K. S. Removal of arsenic in drinking water by iron oxide-coated sand and ferrihydrite-batch studies. *Water Qual. Res. J. Can.* **2001**, *36* (1), 55–70.

(32) Kundu, S.; Kavalakatt, S. S.; Pal, A.; Ghosh, S. K.; Mandal, M.; Pal, T. Removal of arsenic using hardened paste of Portland cement: batch adsorption and column study. *Water Res.* **2004**, *38*, 3780–3790.

(33) Pokhrel, D.; Viraraghavan, T. Arsenic removal from an aqueous solution by modified *A. niger* biomass: batch kinetic and isotherm studies. *J. Hazard. Mater.* **2008**, *150*, 818–825.

(34) Edwards, M. Chemistry of arsenic removal during coagulation and. Fe−Mn oxidation. *J. Am. Water Works Assoc.* **1994**, *86* (9), 64–78.

(35) Huang, C. P.; Vane, L. M. Enhancing As^{5+} removal by a Fe^{2+}-treated activated carbon. *J. Water Pollut. Control Fed.* **1989**, *61* (9), 1596–1603.

(36) Hingston, F. J.; Posner, A. M.; Quirk, J. P. Anion adsorption by goethite and gibbsite. *J. Soil Sci.* **1972**, *23* (2), 177–192.

(37) Sposito, G. The Surface Chemistry of Soils. *The Surface Chemistry of Soils*; Oxford University Press: New York, 1984.

(38) Lagergren, S. About the theory of so-called adsorption of soluble substances. *K. Sven. Vetenskapsakad. Handl.* **1898**, *24* (4), 1–39.

(39) Ho, Y. S.; McKay, G. Kinetic model for lead (II) sorption on to peat. *Adsorpt. Sci. Technol.* **1998**, *16* (4), 243–255.

(40) Joshi, A.; Chaudhuri, M. Removal of Arsenic from Ground Water by Iron Oxide-Coated Sand. *J. Environ. Eng.* **1996**, *122* (8), 769–771.

(41) Kim, Y.; Kim, C.; Choi, I.; Rengaraj, S.; Yi, J. Arsenic removal using mesoporous alumina prepared via a templating method. *Environ. Sci. Technol.* **2004**, *38* (3), 924–931.

(42) Langmuir, I. The constitution and fundamental properties of solids and liquids. *J. Am. Chem. Soc.* **1916**, *38* (11), 2221–2295.

(43) Freundlich, H. M. F. Over the adsorption in solution. *J. Phys. Chem.* **1906**, *57A*, 385.

(44) Mondal, P.; Balomajumder, C.; Mohanty, B. A laboratory study for the treatment of arsenic, iron, and manganese bearing ground water using Fe3+ impregnated activated carbon: Effects of shaking time, pH and temperature. *J. Hazard. Mater.* **2007**, *144* (1−2), 420–426.